Supplement of Atmos. Chem. Phys., 20, 7069–7086, 2020
https://doi.org/10.5194/acp-20-7069-2020-supplement

Atmospheric Chemistry and Physics
Open Access
EGU

Supplement of

Volatile organic compounds and ozone air pollution in an oil production region in northern China

Tianshu Chen et al.

Correspondence to: Likun Xue (xuelikun@sdu.edu.cn)

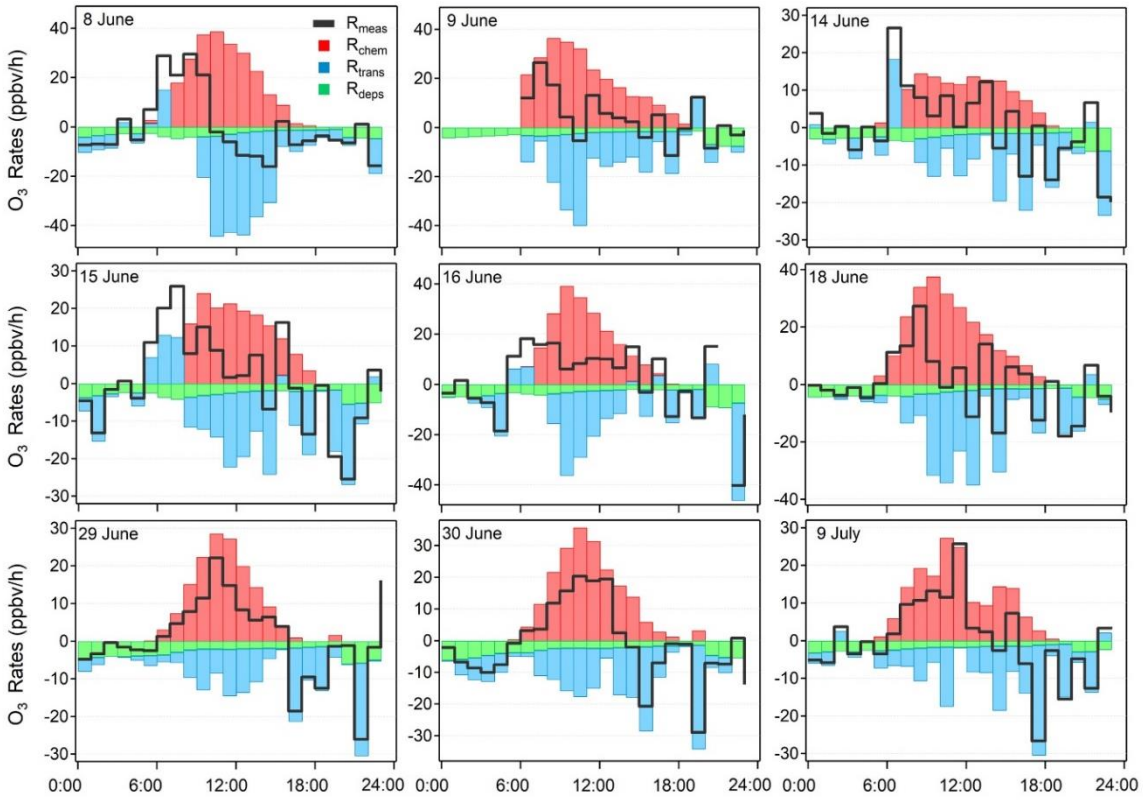

Figure S1. The observed rate of change in O_3 concentrations (R_{meas}) and the contributions from photochemistry (R_{chem}), transport (R_{trans}), and deposition (Rdeps) in the YelRD during the nine selected O_3 episodes.

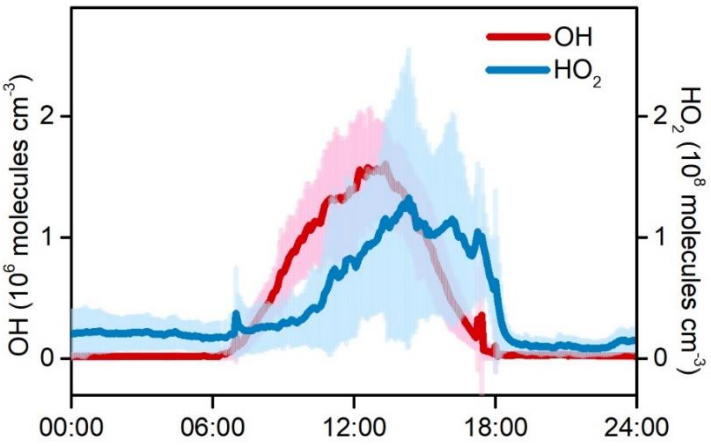

Figure S2. Model-simulated average diurnal variations of OH and HO_2 during the eight selected cases in February-March 2017. The shaded areas indicate the standard deviations of the mean.

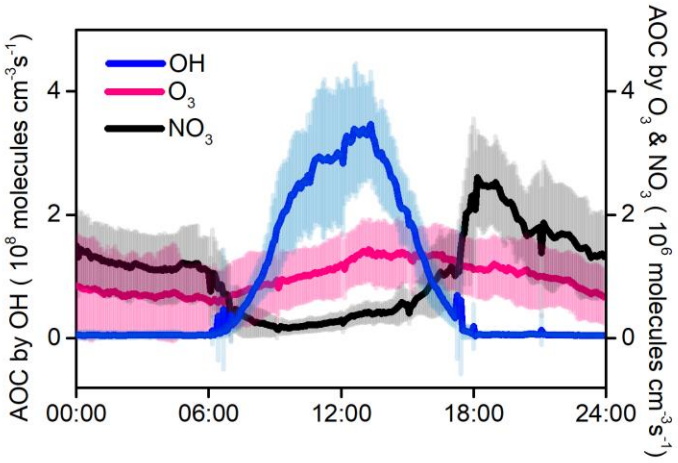

Figure S3. Model-calculated average oxidation capacity of OH, O_3 and NO_3 during the eight selected cases in February-March 2017. The error bars indicate the standard deviations of the mean.

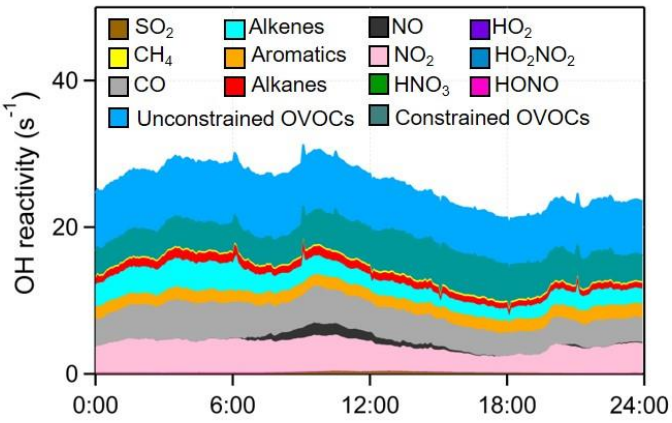

Figure S4. Model-calculated average OH reactivity (K_{OH}) and its breakdown to the major reactants during the eight selected cases in February-March 2017.

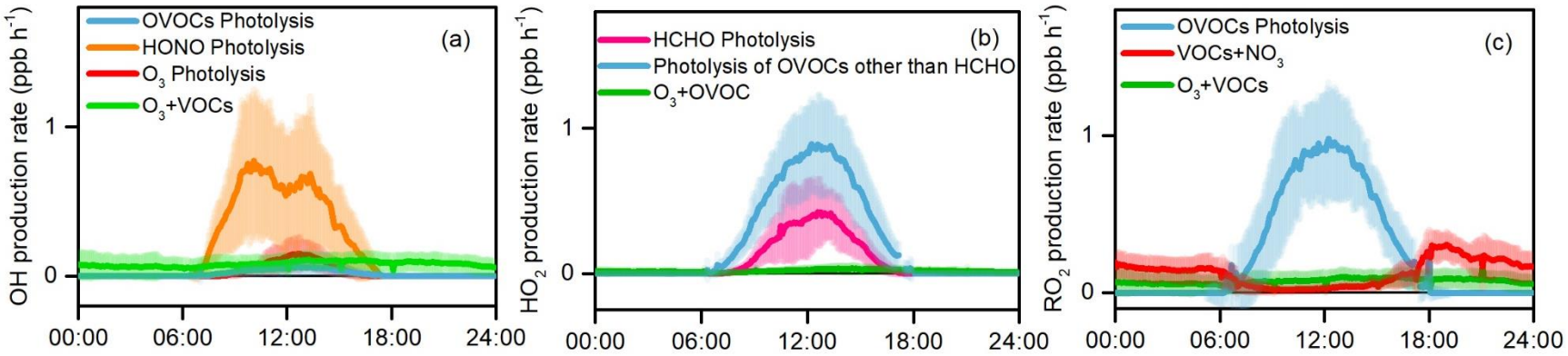

Figure S5. Model-simulated average primary production rates of (a) OH, (b) HO_2, and (c) RO_2 during the eight selected cases in February-March 2017. The error bars indicate the standard deviations of the mean.

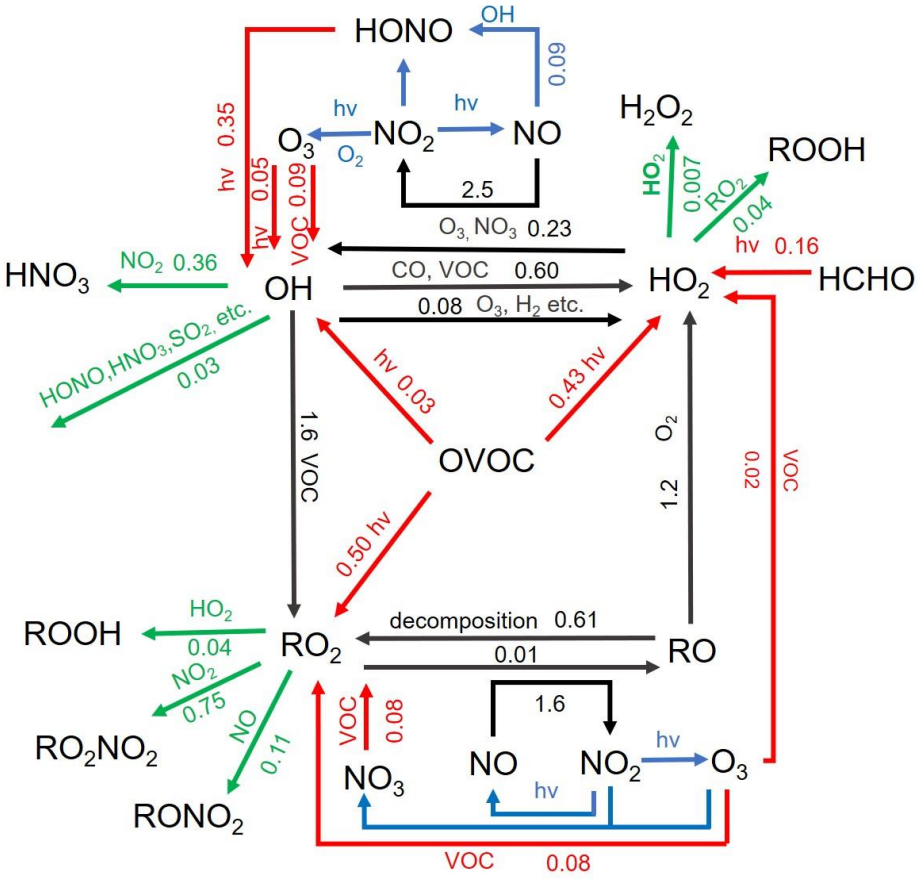

Figure S6. Daytime average (6:00-18:00 LT) RO_x budget during the eight selected cases in February-March 2017. The unit is ppb h^{-1}. The red, green and black lines indicate the production, destruction and recycling pathways of radicals, respectively.

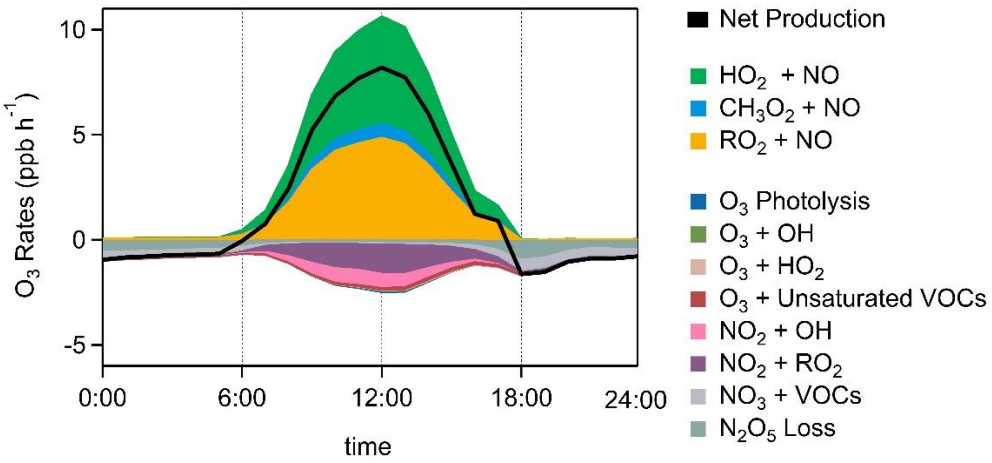

Figure S7. Simulated average O_3 budget during the eight selected cases in February-March 2017.